Precious metal recovery from electronic waste by a porous porphyrin polymer

Yeongran Hong[a], Damien Thirion[b], Saravanan Subramanian[b], Mi Yoo[c], Hyuk Choi[c], Hyun You Kim[c], J. Fraser Stoddart[d,e,f,1], and Cafer T. Yavuz[a,b,g,1]

[a]Department of Chemical and Biomolecular Engineering, Korea Advanced Institute of Science and Technology (KAIST), Yuseong-gu, 34141 Daejeon, Korea; [b]Graduate School of Energy, Environment, Water and Sustainability (EEWS), Korea Advanced Institute of Science and Technology (KAIST), Yuseong-gu, 34141 Daejeon, Korea; [c]Department of Materials Science and Engineering, Chungnam National University, 34134 Daejeon, Korea; [d]Department of Chemistry, Northwestern University, Evanston, IL 60208-3113; [e]Institute of Molecular Design and Synthesis, Tianjin University, 300072 Tianjin, China; [f]School of Chemistry, University of New South Wales, Sydney, NSW 2052, Australia; and [g]Department of Chemistry, Korea Advanced Institute of Science and Technology (KAIST), Yuseong-gu, 34141 Daejeon, Korea

Contributed by J. Fraser Stoddart, May 4, 2020 (sent for review February 4, 2020; reviewed by Sheng Dai, Hani El-Kaderi, and Jonathan L. Sessler)

Urban mining of precious metals from electronic waste, such as printed circuit boards (PCB), is not yet feasible because of the lengthy isolation process, health risks, and environmental impact. Although porous polymers are particularly effective toward the capture of metal contaminants, those with porphyrin linkers have not yet been considered for precious metal recovery, despite their potential. Here, we report a porous porphyrin polymer that captures precious metals quantitatively from PCB leachate even in the presence of 63 elements from the Periodic Table. The nanoporous polymer is synthesized in two steps from widely available monomers without the need for costly catalysts and can be scaled up without loss of activity. Through a reductive capture mechanism, gold is recovered with 10 times the theoretical limit, reaching a record 1.62 g/g. With 99% uptake taking place in the first 30 min, the metal adsorbed to the porous polymer can be desorbed rapidly and reused for repetitive batches. Density functional theory (DFT) calculations indicate that energetically favorable multinuclear-Au binding enhances adsorption as clusters, leading to rapid capture, while Pt capture remains predominantly at single porphyrin sites.

gold reduction | photoreductive recycling | platinum capture | urban mining | water treatment

Electronic devices have become (1–3) an integral part of our human experience and their production to meet the increasing demand generates significant electronic waste (e-waste). A good example is Printed Circuit Boards (PCBs), which amount to around 50 million tons per annum with an 8.8% increase every year (4–6). Although PCBs contain more precious metals than the ores in mines (7), 80% of this waste still goes to landfills (4) chiefly because of the lack of selective, high-yield, noncyanide recovery procedures (6). One current method for urban mining is based on pyrometallurgy (8), which produces hazardous waste (9); this approach is mainly practiced in developing countries (1, 3). Hydrometallurgy (9) can offer the needed selectivity since the use of digestive solutions is more environmentally friendly (10), while biometallurgy approaches remain elusive (11).

The ideal method (3) for precious metal recovery from e-waste, therefore, should entail selective capture from chemically digested solutions without the need for incineration. It has been reported that nitrogen- or sulfur-bearing adsorbents provide the necessary affinity for high-uptake capacities. For example, imidazole immobilized on mesoporous silica and *N,N*-dimethylaminoethyl methacrylate (DMAEMA) covalently bonded onto a commercial polyethylene-coated polypropylene skin-core structure fiber have been reported (12, 13) as precious metal adsorbents. Recently, our team reported (14) that cyclodextrins could coprecipitate with gold ions by forming enzymelike complexes, an approach that could provide an economical means for gold recovery. Zirconium-based metal organic frameworks, such as UiO-66 and UiO-66-NH_2, have also been screened (15) for precious metal uptake.

Biomaterials-based adsorbents, such as cross-linked polysaccharide gels and chemically modified persimmon tannin gels, have been investigated for precious metal recovery (16, 17), with high gold adsorption capacities of 7.57 and 7.7 mmol/g, respectively. Most adsorbents, however, are often tested in pure metal solutions or in the presence of a limited number of competing metals. These protocols, however, have economically less feasible uptake capacities or selectivities and are rarely reported for their applicability in actual e-waste or wastewater. A more targeted approach, employing strongly metal-binding chelators, is needed.

Porphyrins feature (18) remarkably high binding affinity and selectivity for transition metals, particularly the precious metals. Such powerful organic functionalities could, in principle, be employed in permanently porous network polymers in order to immobilize them for the recyclable separation of metals from a complex matrix. Two recent articles, one by our group (19) and another from Dichtel and coworkers (20), focus on removing emerging organic micropollutants from water; neither metals nor porphyrin-containing porous polymers, however, were addressed. The present challenge is to install porphyrins into materials, while using sustainable methods and starting materials.

Reports on chelator-containing porous polymers began (21) with the use of phthalocyanine-containing nanoporous network polymers. While catalysis is usually the application of choice

Significance

Electronic waste, also called e-waste, is rapidly becoming a major industrial hazard because of the increased use of circuits and screens. With the right technology, however, this waste could become a sustainable source for precious metals. Such a solution requires selectivity toward the precious metals, as this characteristic is even more important than capacity. A porphyrin-based porous polymer with selective binding shows remarkable selectivity and a reductive mechanism, a combination which makes for record-high recycling of precious metals—particularly gold—from e-waste.

Author contributions: C.T.Y. designed research; Y.H., M.Y., and H.C. performed research; Y.H., D.T., S.S., and H.Y.K. contributed new reagents/analytic tools; Y.H., D.T., S.S., M.Y., H.C., H.Y.K., J.F.S., and C.T.Y. analyzed data; and J.F.S. and C.T.Y. wrote the paper.

Reviewers: S.D., Oak Ridge National Laboratory; H.E.-K., Virginia Commonwealth University; and J.L.S., University of Texas.

Competing interest statement: KAIST has filed provisional patent applications (KR: 10-2017-0170184, 10-2018-0129227; PCT: PCT/KR2018/013067; US: 16212052; JP: 2018-230885) related to the materials and precious metal recovery reported in this article. J.F.S. and J.L.S. are subcontractors on an NSF CCI grant.

[1]To whom correspondence may be addressed. Email: stoddart@northwestern.edu or yavuz@kaist.ac.kr.

This article contains supporting information online at https://www.pnas.org/lookup/suppl/doi:10.1073/pnas.2000606117/-/DCSupplemental.

First published June 22, 2020.

when utilizing these superstructures (22–29), CO_2 capture and conversion have also been pursued (30–34). Despite the great promise in the use of porphyrins for e-waste treatment, recent progress has been lacking.

In this work, we report a highly porous, exceptionally stable, and very easy-to-build porphyrin network polymer for precious metal capture from e-waste. By linking porphyrins with phenazines, we have imparted the characteristics of robustness and oxidative resistance simultaneously. The covalent organic polymer, COP-180, captures gold at nearly 10 times the theoretical equivalence from a mixture of 63 competing metals. The sorbent can be used multiple times without loss of activity. Even without recycling, we show that the metal-isolation process is economically viable. Density functional theory (DFT) calculations confirm the preferential formation of metal clusters, a necessary mechanism for outstanding gold selectivity.

Results and Discussion

Synthesis of a Porphyrin Network Polymer. A porphyrin-based nanoporous COP (COP-180) was designed and synthesized (Fig. 1) in two steps from commercial building blocks for precious metal recovery from acidic digests of e-waste solutions. After preparing the porphyrin tetranitro monomer ($TNPPH_2$) following literature methods (35) with slight modifications, the nanoporous polymer was synthesized by a Wohl–Aue coupling reaction (36) with phenylenediamine in the presence of KOH. The Brunauer–Emmett–Teller (BET) specific surface area of the synthesized polymer was found to be 704 $m^2\ g^{-1}$ and the polymer shows (Fig. 1*B* and *SI Appendix*, Fig. S1*A*) hierarchical properties with an average pore size of ∼15 nm.

In the Fourier transform infrared spectroscopy (FTIR) spectrum of COP-180, the peaks of =C–H (bending), N–H (bending), C=N (stretch), C=C (stretch), =C–H (stretch), and N–H (stretch) were observed at 796, 967, 1,465, 1,596, 3,030, and 3,371 cm^{-1}, respectively, all common features (18) of a porphyrin macrocycle. The peaks at 1,346 and 1,516 cm^{-1} indicated the existence of unreacted nitro groups in the final product. The 4.7 wt % of oxygen, as determined by elemental analysis, can be associated with the nitro groups and possibly with by-products such as phenazine oxide (*SI Appendix*, Fig. S1*B* and Table S1). The amorphous nature of the polymer was established (*SI Appendix*, Fig. S2) from its powder X-ray diffraction pattern. COP-180 was thermally stable up to almost 400 °C under both nitrogen and air atmosphere (*SI Appendix*, Fig. S3). The nitrogen (1 s) X-ray photoelectron spectroscopy (XPS) spectra of COP-180 show (Fig. 1*D* and *SI Appendix*, Fig. S4) pyrrole nitrogens at the characteristic 397- and 399-eV positions (18) and a peak around 398 eV which arises after metalation.

COP-180 features phenazine linkages (37, 38) and shows exceptional stability under acidic conditions (*SI Appendix*, Fig. S5). The use of Wohl–Aue conditions, however, is also known (39) to give azo adducts. Although azobenzene-based porous polymers were shown previously to be stable enough for CO_2 capture applications by El-Kaderi and coworkers (40) and in our group (41), these polymers cannot withstand aqua regia conditions and therefore were deemed not feasible for e-waste treatment. Despite the low solubility of tetranitrophenyl, porphyrin is expected to lead to a dominant Michael addition for the coupling of monomers and hence the phenazine selectivity (*SI Appendix*, Scheme S1). We prepared a model compound from $TNPPH_2$ and aniline to prove that phenazine formation is preferred. The adduct showed a peak at *m/z* 1,023.4908 in the high-resolution mass spectrum (Fig. 1*C*), indicating quantitative phenazine formation. In addition, we prepared a control polymer that features methyl substituents for suppressing phenazine formation (*SI Appendix*, Scheme S2). The network polymer, dubbed COP-180Azo, was synthesized by following the same reaction procedure as that for COP-180 except for the addition of 2,3,5,6-tetramethylbenzene-1,4-diamine instead of *p*-phenylenediamine to block the phenazine

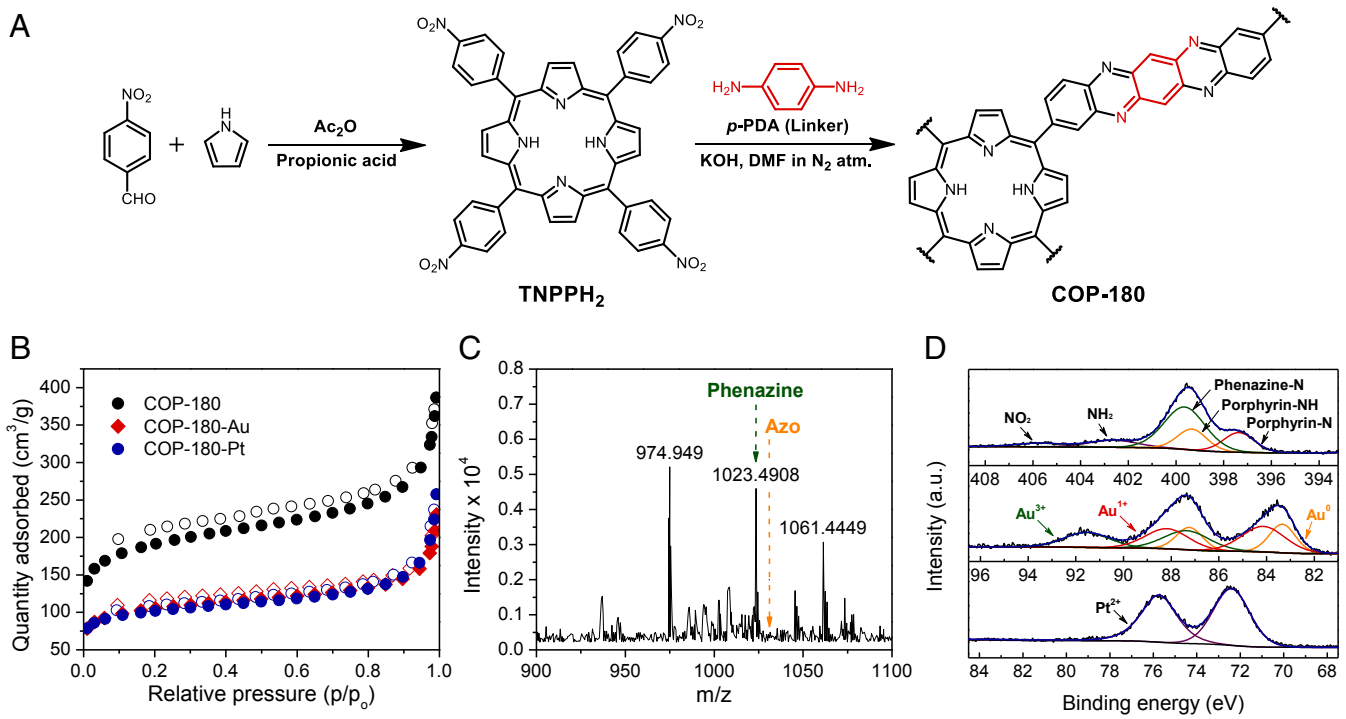

Fig. 1. Synthesis and characterization of COP-180. (*A*) Two-step synthesis of COP-180 from commercially available monomers. (*B*) Nitrogen adsorption–desorption isotherms of COP-180, COP-180-Au, and COP-180-Pt measured at 77 K. Filled and empty symbols represent adsorption and desorption, respectively. (*C*) Matrix-assisted laser desorption/ionization time-of-flight (MALDI-TOF) mass spectrometry analysis of a monomeric model compound confirming phenazine formation. (*D*) XPS spectra of N (1 s) of COP-180, Au (4 f) of Au-loaded polymer, and Pt (4 f) of Pt-loaded polymer.

formation. Formation of the azo linkage was immediately evident from the color changes observed during the synthesis. The resulting product was nonporous and lacked the phenazine carbon signal at 128 ppm in the ^{13}C solid-state cross polarization magic angle spinning (CP/MAS) NMR spectrum (*SI Appendix*, Fig. S1*D*), showing that a substantially different superstructure had resulted. Although the linkage functionality would not ordinarily present a concern for precious metal recovery—since the active adsorption sites are the porphyrin rings we wanted to clarify the structures of the materials. We also prefer phenazine linkages for their outstanding chemical stability.

Porphyrin Network Polymers as Precious Metal Scavengers. Single-metal adsorption efficiencies were tested using a concentrated (3,000 ppm) standardized solution of noble metals. Excessive spiked loading is often used to represent immediate performance with induced saturation. Uptake capacities for gold (21.6%), platinum (13.3%), silver (8.5%), copper (4.1%), and palladium (2.1%) were observed (*SI Appendix*, Table S2). Surprisingly, other competing ions, for example nickel, showed only negligible uptake (0.04%). The BET specific surface areas of metal-loaded COP-180s were decreased, indicating pore-filling behavior (Fig. 1*B* and *SI Appendix*, Fig. S6).

The remarkably high uptake and selectivity for gold and platinum, even at elevated concentrations, prompted us to study them in detail. The gold and platinum adsorption isotherms were collected using standardized solutions in batch conditions and fitted by the Langmuir adsorption isotherm model. Accordingly, the maximum uptake of gold in COP-180 was found to be 1.62 g/g. This value is almost 10 times higher than the value predicted by theory (0.173 g/g), using a scenario in which each porphyrin unit can accommodate only one metal ion. On the contrary, the

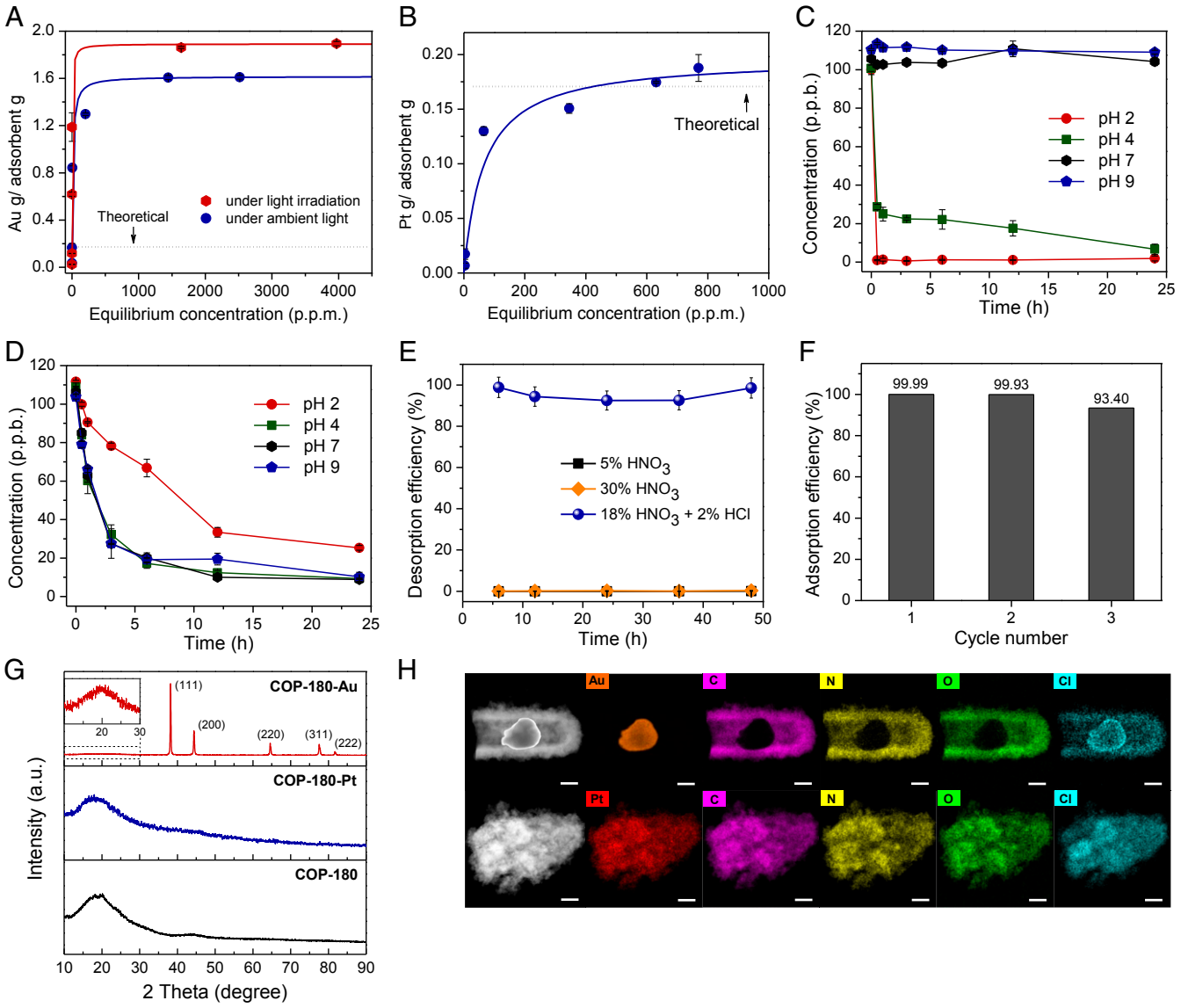

Fig. 2. Precious metal adsorption and desorption of COP-180. (*A*) Gold and (*B*) platinum adsorption isotherms of COP-180. The adsorption isotherms were measured at a pH range of 2–4 for gold and 6–7 for platinum, where the optimized conditions were prepared by dissolving metal salts in water without buffer agents. Time-dependent adsorption efficiencies of (*C*) gold and (*D*) platinum at varying pH values. (*E*) Desorption of gold adsorbed on COP-180 in warm acidic solutions. (*F*) Gold-capture efficiencies for three consecutive adsorption/desorption cycles. (*G*) XRD patterns for Au-loaded, Pt-loaded, and pure COP-180. (*H*) STEM images and elemental mapping for Au (*Upper Row*) and Pt-loaded COP-180 (*Lower Row*). Data are reported as the average uptake of at least three independent experiments. Error bars show minimum and maximum uptake. (Scale bars, 500 nm.)

experimental adsorption amount of platinum in COP-180 was 0.197 g/g (Fig. 2), a value similar to the theoretical capacity of 0.171 g/g.

Mechanism. The unprecedented adsorption of gold ions implies that other adsorptive mechanisms are involved during gold uptake. A viable pathway would therefore be reductive immobilization of gold ions into gold metal clusters, as adsorptive binding would require a similarly high uptake for platinum ions. Phenazines, which are known to be redox-active and are used in biological electron transfer reactions (42), may be responsible for the reductive adsorption in COP-180. In addition, porphyrin and its derivatives are known for their activity as photosensitizers and photoredox catalysts (43). Judging from the ultraviolet/visible (UV/vis) absorption spectrum of COP-180 (*SI Appendix*, Fig. S7), its UV/vis light absorption could induce a photocatalytic reduction of gold (44): $AuCl_4^- + 3e^- \rightarrow Au\ (s) + 4Cl^-\ (aq)$, +1.002 V. Incidentally, the adsorbed amounts of gold (Fig. 2*A* and *SI Appendix*, Fig. S8) were found to be 1.62 g/g under the ambient light and 1.54 g/g in the absence of light. In addition, artificial light irradiation (halogen lamp, 42 W, 630 lm) further increased the gold adsorption capacity of COP-180 (Fig. 2*A*) up to a record 1.89 g/g. In a control experiment, we negated the inevitable heating from the light source by carrying out adsorption in the dark; a capacity of 1.57 g/g at 34 °C resulted.

The X-ray diffraction (XRD) pattern of gold captured within COP-180 displayed elemental gold peaks confirming reductive adsorption (Fig. 2*G*), whereas Pt-loaded COP-180 showed only broad signals from the amorphous porous polymer. Single gold and platinum atoms were observed, and grown crystals of gold in 0.4–1.5-μm sizes were also clearly observed under the electron microscope. Elemental mapping showed (Fig. 2*H* and *SI Appendix*, Fig. S11) clustered gold, while platinum was spread over the entire surface of the adsorbent. Also, the XPS spectrum of Au-loaded COP-180 revealed oxidation states of gold as 0 at 83.99 ($4f_{7/2}$) and 87.89 ($4f_{5/2}$) eV, +1 at 84.78 ($4f_{7/2}$) and 88.83 ($4f_{5/2}$) eV, and +3 at 87.93 ($4f_{7/2}$) and 92.19 ($4f_{5/2}$) eV. Platinum, on the other hand, showed (Fig. 1*D*) only a +2 state at 72.40 ($4f_{7/2}$) and 75.74 ($4f_{5/2}$) eV. Silver is the only other metal that also shows (*SI Appendix*, Figs. S2 and S4) nanoparticle cluster formation, despite the low uptake capacities when compared to gold.

The photocatalytic reaction requires a constant electron supply, and the electron-rich conjugated network of porphyrins and phenazines are thought to meet this requirement. This behavior is particularly evident since reductive adsorption also takes place in the dark, albeit at the decreased capacity of 1.54 g/g. This capacity is, nonetheless, still nine times higher than the theoretical complexation limit. Nitrogen heteroatoms serve both as primary adsorption sites when Pearson's hard–soft acid–base theory (45) is taken into account, and also as reductants, where they are commonly used in nanoparticle synthesis methodologies (46), and where Marcus theory predicts (47) the presence of radical intermediates to form polyamines or nitrous oxides.

The size of the porphyrin cavity (~4.10 Å for free-base porphyrin) is important to consider when describing the capture of divalent ions. It is claimed (18) that if the metal ion size is larger than 80–90 pm, it is more difficult for the ion to enter the ring and, rather, it remains in the sitting-atop form. The ionic radii (44) of platinum (II), palladium (II), and copper (II) are 74, 78, and 71 pm, respectively, and these values match our criteria. Accordingly, these metals are captured in good agreement with ionic radii requirements. Our results also correspond well with the thermodynamic stability of metalloporphyrins, where a trend (18) can be illustrated as follows: Pt (II) > Pd (II) > Ni (II) > Co (II) > Zn (II) > Mg (II) > Cd (II) > Sn (II).

Theoretical Proof of Au Clustering on Porphyrins. We performed spin-polarized DFT calculations with the Vienna Ab initio Simulation Package (48) using the Heyd–Scuseria–Ernzerhof-06 (HSE06) (49) hybrid functional. A single COP-180 unit was used to calculate the binding energy of Au and Pt in COP-180, where the metals were adsorbed sequentially (Fig. 3) at the central N ions of the porphyrin unit to calculate the stepwise binding energy, E_{bind}, of Au and Pt. The results show that Au has a consistent binding energy (−0.67 eV) upon capture of a second Au, whereas Pt is more energetically favorable (–3.10 eV) if only a single Pt is captured. The DFT-calculated data clearly agree with the experimental data, particularly in showing the near-theoretical capture capacity for Pt, while exceeding 10 times theoretical capacity for Au.

The E_{bind} values of Au and Pt were calculated with reference to the Au^{3+} and Pt^{2+} ions, implemented to the system as $AuCl_3$ and $PtCl_2$, respectively. For example, the first E_{bind} was calculated by removing two Cl^- ions of $AuCl_3$ and $PtCl_2$ as gas-phase HCl molecules with the protons of the NH radicals of porphyrin.

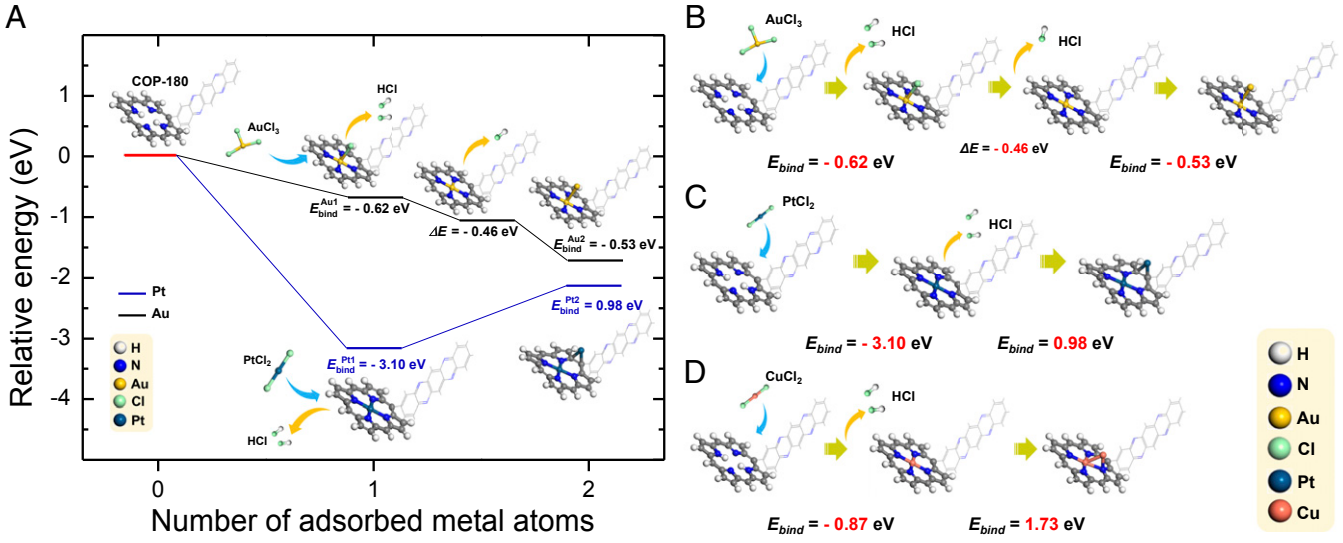

Fig. 3. DFT calculations for Au, Pt, and Cu adsorption on COP-180. (*A*) Spin-polarized DFT calculations for energy changes in multinuclear adsorption of Pt and Au on a model unit of COP-180. (*B*) Energy of binding (E_{bind}) in sequential adsorption of $AuCl_3$, (*C*) $PtCl_2$, and (*D*) $CuCl_2$.

The remaining Cl^- ion of the AuCl was artificially removed by forming a HCl molecule with additionally supplied H atoms.

We found that the porphyrin unit of COP-180 binds strongly a Pt^{2+} ion with E_{bind} of –3.10 eV. The positive E_{bind} of the second binding Pt (0.98 eV) shows, however, that Pt prefers to be atomically separated over porphyrin units because of the lack of the driving force of agglomeration. On the other hand, a stepwise exothermic binding process was observed in Au binding calculations. The E_{bind} of the first binding Au^{3+} ion (E_{bind} = –0.62 eV) was slightly increased up to –0.67 eV for the second bound Au atom, which supplies an exothermic energetic trend, a driving force of Au agglomeration. For copper adsorption, the initial E_{bind} was slightly higher than that of Au (–0.87 eV) but the addition of a second Cu was energetically forbidden (E_{bind} = 1.73 eV, Fig. 3*D*). These findings tailor the experimentally observed inversed trend in elemental distribution of Au and Pt over COP-180, while Cu was the least favored (Fig. 3) in overall total adsorption.

Metal Selectivity and Effects of pH. The adsorption behaviors of Au and Pt also differ under varying pH conditions. At pH 2, 99% of gold ions were removed (Fig. 2 *C* and *D*) within 30 min, while Pt uptake was more sluggish at 77.4% within 24 h. Basic pH adversely affected gold uptake, perhaps as a consequence of gold metal speciation from auryl chloride ions to hydroxide complexes, and the corresponding anionic repulsion with deprotonated porphyrin nitrogens. Near-quantitative recovery of gold was achieved within 6 h by using a mixture of dilute HNO_3 and HCl at warm temperatures. Gold adsorption and desorption trials were then repeated (Fig. 2 *E* and *F*) three times with the maintained adsorption efficiencies of more than 93%.

Competing Metals Test. E-waste contains (*SI Appendix*, Table S3) a large amount of common metals such as sodium, copper, tin, zinc, and iron in an acid digest (10) and selectivity, in low concentrations, is the ultimate test for a proposed adsorbent. For this purpose, we chose multielement standard solutions commonly used

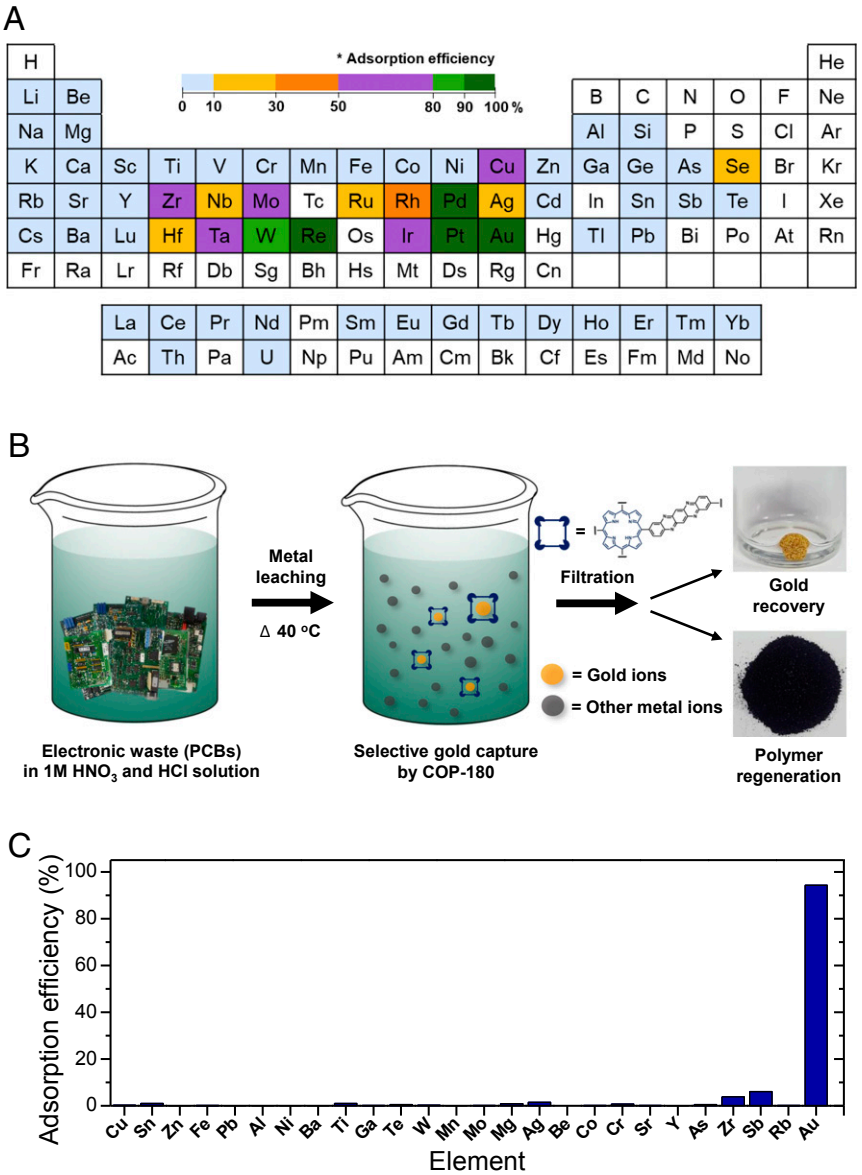

Fig. 4. Testing COP-180 in a mixture containing all common metals in the Periodic Table and gold capture from actual electronic circuit boards. (*A*) Mixed-metal selectivity test results summarized on a periodic table. (*B*) Real-life application of COP-180 for gold recovery from PCBs. The gold ingot is >99.6% pure. (*C*) Corresponding adsorption efficiencies of metals that are found in PCBs.

for inductively coupled plasma mass spectrometry (ICP-MS), since they contain a variety of metals in a single solution with calibrated concentrations. The COP-180 was treated (Fig. 4*A* and *SI Appendix*, Table S4) with four different standard solutions covering almost all common metals in the Periodic Table. From direct competition of all metals in acidic solution, precious metals such as platinum (99.8%), palladium (99.8%), and gold (99.4%) were found to be captured selectively. Other precious metals also showed relatively high or moderate adsorption efficiencies; these included iridium (68.9%), rhodium (63.3%), ruthenium (40.4%), copper (12.4%), and silver (24.8%).

In a parallel experiment, COP-180 was treated with combination of two or more standard mixed-metal solutions. The metal adsorption efficiencies in these experiments were found to be almost maintained, or even higher than before, with the values of 99.7, 99.4, and 98.8, 62.5, 59.0, 43.4, and 17.7% for platinum, palladium, and gold, iridium, copper, rhodium, and ruthenium (*SI Appendix*, Fig. S9), respectively. Most of the common elements in the solution showed low adsorption efficiencies of less than 3%. These results indicate that the synthesized COP-180 can be used effectively for the purpose of recovering precious metals from mixed-metal solutions.

Authentic e-Waste Gold Capture Test and Economics. The ultimate test for COP-180 was to verify the applicability of COP-180 in acid-digested e-waste for precious metal recovery (Fig. 4*B*). Seven PCBs were collected from junkyards and treated with dilute aqua regia. The digests were filtered and adjusted to pH ∼2 by adding KOH. COP-180 was added to the metal leachate and the solution was stirred vigorously at room temperature. After filtration, COP-180 was analyzed for metal content. Gold was found (Fig. 4*C*) to be captured with 94% efficiency. We attribute this result to the reductive adsorption process that we observed previously with pure metal isotherms. Upon recovery of the captured gold, a small gold ingot (>99.6% purity) was formed (Fig. 4*B*) in the vial.

Lastly, we calculated the rough economics of gold recovery from PCBs, as e-waste recycling in the commercial sector would be driven by the profits of precious metal recovery and resale. COP-180 was found to cost $5/g based on its chemical starting materials (*SI Appendix*, Table S6), while the gold captured by 1 g of COP-180 would be worth approximately $64. The cost of the polymer is in line with our previous estimates of other porous polymers (50–52). The profit margin can be expected to increase significantly across each subsequent recycling operation, although single-use gold extraction appears to be economically viable.

Materials and Methods

Detailed experimental procedures and characterization can be found in *SI Appendix*.

Synthesis of COP-180. The porphyrin monomer, 5,10,15,20-Tetrakis(4-nitrophenyl)-21H,23H-porphyrin (1 g), *p*-phenylenediamine (275 mg), and KOH (710 mg) were added to dry DMF (200 mL). The mixture was stirred for 1 h under nitrogen purge. The mixture was heated to 150 °C and refluxed for 24 h under a N_2 atmosphere. After cooling to room temperature, the reaction mixture was poured into 1 L of deionized (DI) water and stirred for 1 h. The precipitate was collected by filtration and purified by Soxhlet extraction with water and acetone for 1 d each. The product was dried at 150 °C for 1 d in a vacuum oven. Yield: 75%.

Precious Metal Capture from Actual e-Waste. PCBs were obtained from the local junk shop. First, the PCBs were soaked in 10 M of NaOH solution for 1 d to remove the surface epoxy coating. The PCBs were removed from the basic solution and washed with tap water before soaking them in 4 L of an HNO_3/HCl (1 M each) solution. The temperature of the solution was raised to 40 °C and held for 2 d. The PCBs were taken out and the acidic solution was filtered to remove any undissolved components. Sufficient KOH was added to the solution to give a positive pH value, and DI water was added to give a 5 L final solution. COP-180 (1 g) was added to the solution and the mixture was stirred for 2 d. After filtering, the COP-180 was washed thoroughly with DI water. The metals adsorbed on COP-180 were analyzed by ICP-MS and their amounts were compared with the metal concentrations of the solution before COP-180 addition.

Data Availability. All procedures and results of experiments are described in detail in the main text and *SI Appendix*.

ACKNOWLEDGMENTS. This research was supported primarily by Nano-Material Technology Development Program through the National Research Foundation of Korea (NRF) funded by the Ministry of Science, ICT and Future Planning (2017M3A7B4042140 and NRF-2017M3A7B4042235). Funds from NRF (NRF-2016R1A2B4011027) are also gratefully acknowledged. J.F.S. is funded by the Center for Sustainable Separation of Metals, an NSF Center for Chemical Innovation (CCI) Grant CHE-1925708. This research used resources of the Center for Functional Nanomaterials, which is a US Department of Energy Office of Science Facility, and the Scientific Data and Computing Center, a component of the Computational Science Initiative, at Brookhaven National Laboratory under Contract DE-SC0012704. We thank Dr. Margaret E. Schott of Northwestern University for assistance with editing.

1. D. N. Perkins, M.-N. Brune Drisse, T. Nxele, P. D. Sly, E-waste: A global hazard. *Ann. Glob. Health* **80**, 286–295 (2014).
2. B. K. Reck, T. E. Graedel, Challenges in metal recycling. *Science* **337**, 690–695 (2012).
3. M. P. O'Connor, J. B. Zinnerman, P. T. Anastas, D. L. Plata, A strategy for material supply chain sustainability: Enabling a circular economy in the electronics industry through green engineering. *ACS Sustain. Chem. Eng.* **4**, 5879–5888 (2016).
4. B. Ghosh, M. K. Ghosh, P. Parhi, P. S. Mukherjee, B. K. Mishra, Waste printed circuit boards recycling: An extensive assessment of current status. *J. Clean. Prod.* **94**, 5–19 (2015).
5. J. Cui, L. Zhang, Metallurgical recovery of metals from electronic waste: A review. *J. Hazard. Mater.* **158**, 228–256 (2008).
6. A. Akcil *et al*., Precious metal recovery from waste printed circuit boards using cyanide and non-cyanide lixiviants–A review. *Waste Manag.* **45**, 258–271 (2015).
7. Y. Lu, Z. Xu, Precious metals recovery from waste printed circuit boards: A review for current status and perspective. *Resour. Conserv. Recycling* **113**, 28–39 (2016).
8. W. J. Hall, P. T. Williams, Separation and recovery of materials from scrap printed circuit boards. *Resour. Conserv. Recycling* **51**, 691–709 (2007).
9. Z. Sun *et al*., Toward sustainability for recovery of critical metals from electronic waste: The hydrochemistry processes. *ACS Sustain. Chem. Eng.* **5**, 21–40 (2017).
10. U. Jadhav, H. Hocheng, Hydrometallurgical recovery of metals from large printed circuit board pieces. *Sci. Rep.* **5**, 14574 (2015).
11. W.-Q. Zhuang *et al*., Recovery of critical metals using biometallurgy. *Curr. Opin. Biotechnol.* **33**, 327–335 (2015).
12. T. Kang, Y. Park, K. Choi, J. S. Lee, J. Yi, Ordered mesoporous silica (SBA-15) derivatized with imidazole-containing functionalities as a selective adsorbent of precious metal ions. *J. Mater. Chem.* **14**, 1043–1049 (2004).
13. X. Y. Liu *et al*., Green and efficient synthesis of an adsorbent fiber by preirradiation-induced grafting of PDMAEMA and its Au(III) adsorption and reduction performance. *J. Appl. Polym. Sci.* **134**, 44955 (2017).
14. Z. Liu *et al*., Selective isolation of gold facilitated by second-sphere coordination with α-cyclodextrin. *Nat. Commun.* **4**, 1855 (2013).
15. S. Lin *et al*., Effective adsorption of Pd(II), Pt(IV) and Au(III) by Zr(IV)-based metal-organic frameworks from strongly acidic solutions. *J. Mater. Chem. A* **5**, 13557–13564 (2017).
16. B. Pangeni *et al*., Selective recovery of gold using some cross-linked polysaccharide gels. *Green Chem.* **14**, 1917–1927 (2012).
17. M. Gurung *et al*., Recovery of Au(III) by using low cost adsorbent prepared from persimmon tannin extract. *Chem. Eng. J.* **174**, 556–563 (2011).
18. D. Dolphin, *The Porphyrins*, (Academic, New York, 1978).
19. J. Byun, H. A. Patel, D. Thirion, C. T. Yavuz, Charge-specific size-dependent separation of water-soluble organic molecules by fluorinated nanoporous networks. *Nat. Commun.* **7**, 13377 (2016).
20. A. Alsbaiee *et al*., Rapid removal of organic micropollutants from water by a porous β-cyclodextrin polymer. *Nature* **529**, 190–194 (2016).
21. N. B. McKeown, S. Makhseed, P. M. Budd, Phthalocyanine-based nanoporous network polymers. *Chem. Commun.* **23**, 2780–2781 (2002).
22. K. Zhang, O. K. Farha, J. T. Hupp, S. T. Nguyen, Complete double epoxidation of divinylbenzene using Mn(porphyrin)-based porous organic polymers. *ACS Catal.* **5**, 4859–4866 (2015).
23. G. Mukherjee *et al*., A porous porphyrin organic polymer (PPOP) for visible light triggered hydrogen production. *Chem. Commun.* **53**, 4461–4464 (2017).
24. X. Feng *et al*., High-rate charge-carrier transport in porphyrin covalent organic frameworks: Switching from hole to electron to ambipolar conduction. *Angew. Chem. Int. Ed.* **51**, 2618–2622 (2012).
25. S. Wan *et al*., Covalent organic frameworks with high charge carrier mobility. *Chem. Mater.* **23**, 4094–4097 (2011).

26. L. Zou *et al*., Facile one-pot synthesis of porphyrin based porous polymer networks (PPNs) as biomimetic catalysts. *Chem. Commun.* **51**, 4005–4008 (2015).
27. G. Lu *et al*., Metallated porphyrin based porous organic polymers as efficient electrocatalysts. *Nanoscale* **7**, 18271–18277 (2015).
28. S. Brüller *et al*., Bimetallic porous porphyrin polymer-derived non-precious metal electrocatalysts for oxygen reduction reactions. *J. Mater. Chem. A* **3**, 23799–23808 (2015).
29. J. Jiang, S. Yoon, A metalated porous porphyrin polymer with $[Co(CO)_4]^-$ anion as an efficient heterogeneous catalyst for ring expanding carbonylation. *Sci. Rep.* **8**, 13243 (2018).
30. V. S. P. K. Neti, X. Wu, S. Deng, L. Echegoyen, Selective CO_2 capture in an imine linked porphyrin porous polymer. *Polym. Chem.* **4**, 4566–4569 (2013).
31. A. Modak, M. Nandi, J. Mondal, A. Bhaumik, Porphyrin based porous organic polymers: Novel synthetic strategy and exceptionally high CO_2 adsorption capacity. *Chem. Commun.* **48**, 248–250 (2012).
32. S. Lin *et al*., Covalent organic frameworks comprising cobalt porphyrins for catalytic CO_2 reduction in water. *Science* **349**, 1208–1213 (2015).
33. Z. Tian, S. Dai, D.-E. Jiang, Expanded porphyrins as two-dimensional porous membranes for CO_2 separation. *ACS Appl. Mater. Interfaces* **7**, 13073–13079 (2015).
34. X.-S. Wang *et al*., A porous covalent porphyrin framework with exceptional uptake capacity of saturated hydrocarbons for oil spill cleanup. *Chem. Commun.* **49**, 1533–1535 (2013).
35. A. Bettelheim, B. A. White, S. A. Raybuck, R. W. Murray, Electrochemical polymerization of amino-substituted, pyrrole-substituted, and hydroxy-substituted tetraphenylporphyrins. *Inorg. Chem.* **26**, 1009–1017 (1987).
36. A. Wohl, W. Aue, Ueber die einwirkung von nitrobenzol auf anilin bei gegenwart von alkali. *Ber. Dtsch. Chem. Ges.* **34**, 2442–2450 (1901).
37. J. Guo *et al*., Conjugated organic framework with three-dimensionally ordered stable structure and delocalized π clouds. *Nat. Commun.* **4**, 2736 (2013).
38. K. Jie *et al*., A benzoquinone-derived porous hydrophenazine framework for efficient and reversible iodine capture. *Chem. Commun.* **54**, 12706–12709 (2018).
39. H. A. Patel *et al*., Unprecedented high-temperature CO_2 selectivity in N_2-phobic nanoporous covalent organic polymers. *Nat. Commun.* **4**, 1357 (2013).
40. P. Arab, M. G. Rabbani, A. K. Sekizkardes, T. İslamoğlu, H. M. El-Kaderi, Copper(I)-catalyzed synthesis of nanoporous azo-linked polymers: Impact of textural properties on gas storage and selective carbon dioxide capture. *Chem. Mater.* **26**, 1385–1392 (2014).
41. H. A. Patel *et al*., Directing the structural features of N_2-phobic nanoporous covalent organic polymers for CO_2 capture and separation. *Chem. Eur. J.* **20**, 772–780 (2014).
42. A. Hollas *et al*., A biomimetic high-capacity phenazine-based anolyte for aqueous organic redox flow batteries. *Nat. Energy* **3**, 508–514 (2018).
43. K. Rybicka-Jasińska, W. Shan, K. Zawada, K. M. Kadish, D. Gryko, Porphyrins as photoredox catalysts: Experimental and theoretical studies. *J. Am. Chem. Soc.* **138**, 15451–15458 (2016).
44. W. M. Haynes, D. R. Lide, *CRC Handbook of Chemistry and Physics: A Ready-Reference Book of Chemical and Physical Data*, (CRC Press, Boca Raton, FL, 2011).
45. R. G. Pearson, Hard and soft acids and bases – The evolution of a chemical concept. *Coord. Chem. Rev.* **100**, 403–425 (1990).
46. X. Lu, H. Y. Tuan, B. A. Korgel, Y. Xia, Facile synthesis of gold nanoparticles with narrow size distribution by using AuCl or AuBr as the precursor. *Chem. Eur. J.* **14**, 1584–1591 (2008).
47. J. D. S. Newman, G. J. Blanchard, Formation of gold nanoparticles using amine reducing agents. *Langmuir* **22**, 5882–5887 (2006).
48. G. Kresse, J. Furthmüller, Efficient iterative schemes for ab initio total-energy calculations using a plane-wave basis set. *Phys. Rev. B Condens. Matter* **54**, 11169–11186 (1996).
49. A. V. Krukau, O. A. Vydrov, A. F. Izmaylov, G. E. Scuseria, Influence of the exchange screening parameter on the performance of screened hybrid functionals. *J. Chem. Phys.* **125**, 224106 (2006).
50. S. Subramanian *et al*., Catalytic non-redox carbon dioxide fixation in cyclic carbonates. *Chem* **5**, 3232–3242 (2019).
51. V. Rozyyev *et al*., High-capacity methane storage in flexible alkane-linked porous aromatic network polymers. *Nat. Energy* **4**, 604–611 (2019).
52. U. Jeong *et al*., Inversion of dispersion: Colloidal stability of calixarene modified metal-organic framework nanoparticles in non-polar media. *J. Am. Chem. Soc.* **141**, 12182–12186 (2019).